

Influence of thickness on current-induced magnetization switching in $L1_0$-FePt single layer

Shi-Qi Zheng(郑诗琪), Kang-Kang Meng(孟康康), Zhen-Guo Fu(付振国), Ji-Kun Chen(陈吉堃), Jun Miao(苗君), Xiao-Guang Xu(徐晓光), and Yong Jiang(姜勇)

Citation: Chin. Phys. B, 2021, 30 (**10**): 107101. DOI: 10.1088/1674-1056/ac0a62
Journal homepage: http://cpb.iphy.ac.cn; http://iopscience.iop.org/cpb

What follows is a list of articles you may be interested in

Magnetic impurity in hybrid and type-II nodal line semimetals

Xiao-Rong Yang(杨晓容), Zhen-Zhen Huang(黄真真), Wan-Sheng Wang(王万胜), and Jin-Hua Sun(孙金华)
Chin. Phys. B, 2021, 30 (**6**): 067103. DOI: 10.1088/1674-1056/abfa02

Two-dimensional hexagonal Zn_3Si_2 monolayer: Dirac cone material and Dirac half-metallic manipulation

Yurou Guan(官雨柔), Lingling Song(宋玲玲), Hui Zhao(赵慧), Renjun Du(杜仁君), Liming Liu(刘力铭), Cuixia Yan(闫翠霞), Jinming Cai(蔡金明)
Chin. Phys. B, 2020, 29 (**8**): 087103. DOI: 10.1088/1674-1056/ab943a

Giant interface spin-orbit torque in NiFe/Pt bilayers

Shu-Fa Li(李树发), Tao Zhu(朱涛)
Chin. Phys. B, 2020, 29 (**8**): 087102. DOI: 10.1088/1674-1056/ab9292

Global phase diagram of a spin-orbit-coupled Kondo lattice model on the honeycomb lattice

Xin Li(李欣), Rong Yu(俞榕), Qimiao Si
Chin. Phys. B, 2019, 28 (**7**): 077102. DOI: 10.1088/1674-1056/28/7/077102

Graphene-like Be_3X_2 (X=C, Si, Ge, Sn): A new family of two-dimensional topological insulators

Lingling Song(宋玲玲), Lizhi Zhang(张礼智), Yurou Guan(官雨柔), Jianchen Lu(卢建臣), Cuixia Yan(闫翠霞), Jinming Cai(蔡金明)
Chin. Phys. B, 2019, 28 (**3**): 037101. DOI: 10.1088/1674-1056/28/3/037101

Influence of thickness on current-induced magnetization switching in $L1_0$-FePt single layer*

Shi-Qi Zheng(郑诗琪)[1], Kang-Kang Meng(孟康康)[1,†], Zhen-Guo Fu(付振国)[2], Ji-Kun Chen(陈吉堃)[1], Jun Miao(苗君)[1], Xiao-Guang Xu(徐晓光)[1], and Yong Jiang(姜勇)[1,‡]

[1] *School of Materials Science and Engineering, University of Science and Technology Beijing, Beijing* 100083, *China*
[2] *Institute of Applied Physics and Computational Mathematics, Beijing* 100083, *China*

(Received 6 March 2021; revised manuscript received 7 June 2021; accepted manuscript online 11 June 2021)

The thickness dependent spin–orbit torque (SOT) in an $L1_0$-FePt single layer is investigated in this work. As the thickness increases from 8 nm to 16 nm, the magnetization switching ratio in the $L1_0$-FePt film with higher chemical ordering becomes smaller. It is noted that compared with 3-nm-thick $L1_0$-FePt film, 8-nm-thick $L1_0$-FePt film can switch much magnetization with the increase of chemical ordering. When the FePt film is thick enough, the SOT in FePt is closely related to the $L1_0$-ordered structure, which indicates a bulk nature. Therefore, the disordering plays an important role in the magnetization switching only for the ultra-thin FePt films, while the structural gradient may play an important role for thicker films. However, both of the two mechanisms cannot fully explain the process of magnetization switching and the spin current generation. Although many factors influence SOT, here in this work we emphasize only the bulk nature of strong SOC in $L1_0$-FePt through density functional theory calculations, which should generate large spin current due to spin Hall effect.

Keywords: spin–orbit coupling, magnetic anisotropy, spin transport effects

PACS: 71.70.Ej, 71.70.Ej, 75.76.+j **DOI:** 10.1088/1674-1056/ac0a62

1. Introduction

In order to read or write the information in advanced technologies such as magnetic random access memories (MRAMs), it is necessary to achieve a fast magnetization reversal. In a conventional MRAM, the magnetization is switched by the magnetic fields created by currents in nearby conductors, which are known as Oersted fields. However, nowadays, many research laboratories are dedicated to investigating current-driven magnetic dynamics since it is more effective to switch magnetization by spin-torques rather than magnetic field. In ferromagnetic materials or heterostructures, the electronic carriers can transfer their angular momentum to the lattice through spin current, leading to spin-torques, and the transfer rate is equal to the rate of change of angular momentum in the lattice. In the past few years, the current induced magnetization switching in magnetic materials and heterostructures with strong spin–orbit coupling (SOC) presented a new way to read and write information by the spin–orbit torque (SOTs). It can provide efficient technique to switch magnetization in many classes of materials, including ferromagnets (FM),[1–4] antiferromagnets,[5,6] ferrimagnets,[7] magnetic insulators,[8] and magnetic multilayers.[9] In these material systems, even an initially unpolarized current can produce an exert torque, if it becomes spin polarized via spin Hall effect (SHE) or Rashba–Edelstein effect.[10–16] When an electric current passes through a material that contains spin–orbit scatterers, there can be a spin accumulation at the surface. The spin–orbit scatters originate from intrinsic or interfacial SOC, which is known as the SHE or the Rashba–Edelstein effect respectively.[17–25]

Currently, the researches of SOT focus mainly on FM/HM bilayer (or multilayer) structures.[26,27] However, it largely restricts the selection of materials for the practical application. To cope with these issues, studies about SOT in single FM layers have attracted more and more attention.[28,29] For practical applications, the bulk perpendicular magnetic anisotropy (PMA) $L1_0$-FePt has been widely used as a permanent magnet in many kinds of instruments where its exceptional corrosion resistance, ductility, machinability and good high-temperature performance justify the high cost.[30–32] On the other hand, an efficient magnetization switching is highly desirable for the further advancing of modern information technologies. Recently, we have investigated the self-induced SOT in the $L1_0$-FePt single layer with the same thickness (3 nm) but with different disordering. We have found that nearly full magnetization switching happens only in more disordered films, and the magnetization switching ratio becomes smaller with increasing $L1_0$ ordering.[33] However, Tang *et al.* have also found self-induced SOT in the $L1_0$-FePt single layer,

*Project supported by the National Key Research and Development Program of China (Grant No. 2019YFB2005801), the National Natural Science Foundation of China (Grant Nos. 51971027, 51731003, 51971023, 51927802, and 51971024), and the Fundamental Research Funds for the Central Universities, China (Grant No. FRF-TP-19-001A3).

†Corresponding author. E-mail: kkmeng@ustb.edu.cn
‡Corresponding author. E-mail: yjiang@ustb.edu.cn

© 2021 Chinese Physical Society and IOP Publishing Ltd

but they have ascribed it to the composition gradient along the normal direction of the film.[34] Therefore, the mechanisms for magnetization switching are far from fully studied.

In this work, we further investigate the SOT of the $L1_0$-FePt single layer with different thickness and growth temperatures. We find that the magnetization switching ratio in $L1_0$-FePt film with high chemical ordering becomes smaller with thickness increasing from 8 nm to 16 nm. It is noted that compared with 3-nm-thick $L1_0$-FePt film, 8-nm-thick $L1_0$-FePt film can switch much magnetization with the increase of chemical ordering. When the FePt film is thick enough, the SOT in FePt is closely related to the $L1_0$-ordered structure, which indicates a bulk nature. Therefore, the disordering plays an important role in the magnetization switching only for the ultra-thin FePt films, while the structural gradient may play an important role for thicker films. However, both of the two mechanisms cannot fully explain the process of magnetization switching and the spin current generation. Although many factors influence SOT, here in this work we emphasize only the bulk nature of strong SOC in $L1_0$-FePt through density functional theory calculations, which should generate large spin current due to SHE.

2. Materials and methods

The $L1_0$-ordered FePt films with different thickness were epitaxially grown on MgO (001) substrates by high vacuum magnetron sputtering, in which the Fe and Pt atoms were sputtered simultaneously by co-sputtering from Fe and Pt elemental targets at an elevated temperature. After deposition, the samples were annealed by 2 h *in situ* at the same temperature to promote the formation of the $L1_0$ phase of FePt alloy, and then the films are cooled down to room temperature *in situ*. In order to prepare FePt films with different chemical ordering, the growth temperature T_g is adjusted in a range from 350 °C to 450 °C for different samples in our study.

3. Results and discussion

The different thickness of $L1_0$-FePt films with T_g = 450 °C are confirmed by x-ray reflectivity (XRR) as shown in Fig. 1(a). And the roughness values of films are all less than 0.31 nm from the results of XRR. Figure 1(b) shows the structure characterization of these four samples through x-ray diffraction (XRD) measurements. As shown in Fig. 1(b), with the thicknesses increasing, the fct (001) and the fct (002) peak in the spectrum of FePt film become more obvious. The chemical ordering S can be calculated from the intensities of (001) peak and (002) peak.[33,35] The values for these four samples with different thicknesses are all higher than 0.75, indicating the high chemical ordering. Figure 1(c) shows the magnetic hysteresis loops for 16-nm-thick $L1_0$-FePt film at T_g = 450 °C, measured by VSM, which shows an evident bulk PMA. The saturated magnetization $\boldsymbol{M}_S$ and the coercivity fields $\boldsymbol{H}_C$ of the $L1_0$-FePt films with different thicknesses at T_g = 450 °C are shown in Fig. 1(d). The $\boldsymbol{M}_S$ keeps around 1000 emu/cc–1050 emu/cc with varying thickness, and the $\boldsymbol{H}_C$ decreases with the thickness increasing, which may stem from the weaker pinning effect due to lower defect density for thicker FePt.[34]

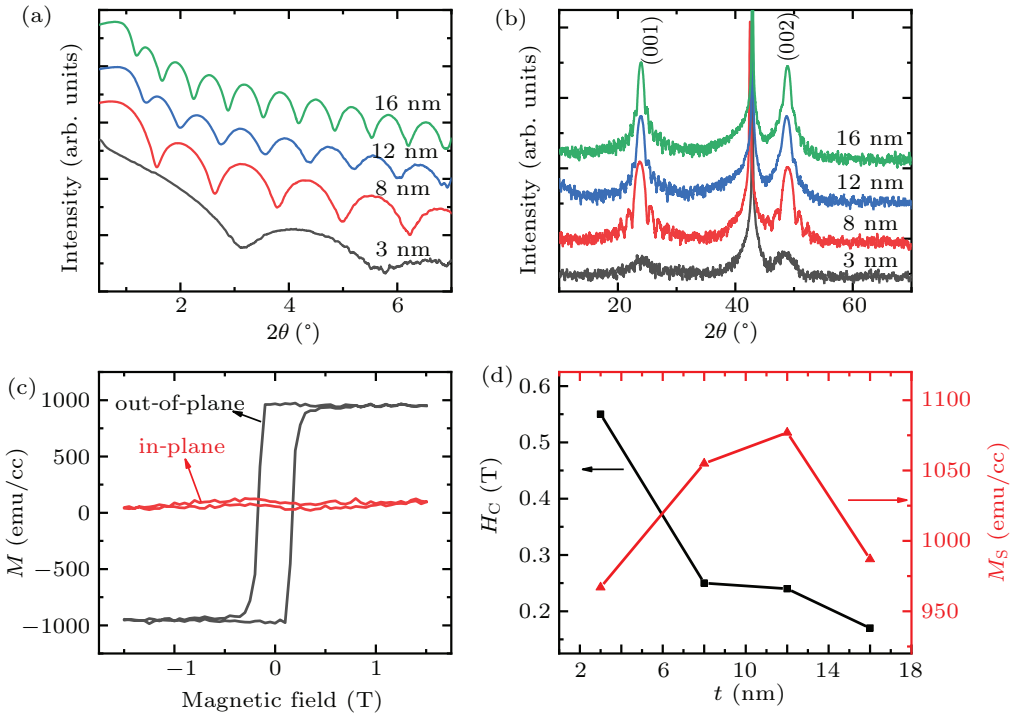


Fig. 1. (a) Curves of x-ray reflectivity of $L1_0$-FePt films grown at 450 °C with different thicknesses. (b) XRD patterns of $L1_0$-FePt films grown at 450 °C with different thicknesses. (c) In-plane and out-of-plane magnetic hysteresis loop of 16-nm-thick $L1_0$-FePt film grown at 450 °C. (d) $\boldsymbol{M}_S$ and $\boldsymbol{H}_C$ *versus* thickness of the $L1_0$-FePt films grown at 450 °C.

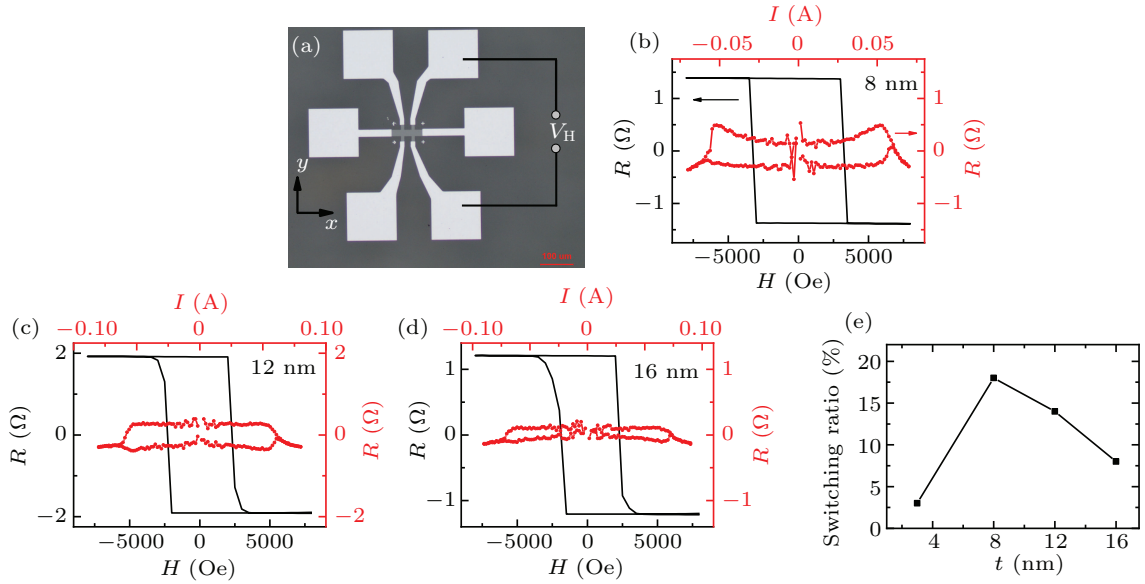


Fig. 2. (a) SEM image of Hall bar along with the definition of the coordinate system used in this study. (b)–(d) Magnetic field dependence of anomalous Hall resistance (*R*–*H*) and current-induced magnetization switching behaviors (*R*–*I*) for $L1_0$ FePt films grown at 450 °C with varying thickness from 8 nm to 16 nm. (e) Magnetization switching ratio *versus* thickness. The unit 1 Oe = 79.5775 A·nm^{-1}.

After depositions, the films are prepared into Hall bar devices for electrical measurement by using electron beam lithography and Ar ion milling. The scan electron microscopy (SEM) image of the Hall bar of 20 μm×120 μm along with the definition of the coordinate system used in our study is shown in Fig. 2(a). The current-induced magnetization switching behaviors in $L1_0$-FePt films with different thicknesses are measured by using a non-zero in-plane field along the *X* direction. The current-induced switching loops are compared with the loops of magnetic field dependence of anomalous Hall resistance at room temperature, and the results are shown in Figs. 2(b)–2(d). Compared with the Hall resistance, only a partial magnetization can be found to be switched in the $L1_0$-FePt films.

We summarize the variation trend of magnetization switching ratio with thickness as shown in Fig. 2(e). It is found that smaller part of magnetization can be switched with thickness increasing, except for the ultra-thin $L1_0$-FePt film (3 nm). In our previous study, the SOT in ultra-thin $L1_0$-FePt films was investigated,[33] in which we found that nearly full magnetization switching happens only in more disordered films, and the magnetization switching ratio becomes smaller with the increase of $L1_0$ ordering.[33] Here, with thickness increasing, the structural gradient as discussed by Tang *et al.* can play a more important role, where the current-induced magnetization switching efficiency and the quantified effective magnetic fields increase with the augment of film thickness and chemical ordering in FePt.[34] Therefore, the switching ratio is higher in 8-nm-thick film than in 3-nm-thick film. However, with further increasing thickness, the switching ratio decreases as shown in Fig. 2(e), which is opposite to the results in Ref. [34]. It indicates that more factors should be taken into consideration for SOT of single $L1_0$-FePt film. Here, the possible mechanisms result from the difference in different interfacial strain and grain sizes of FePt films with varying thickness. The reduced grain size in relatively thin film can lead to lower energy barrier for domain nucleation, thereby enhancing the switching ratio.

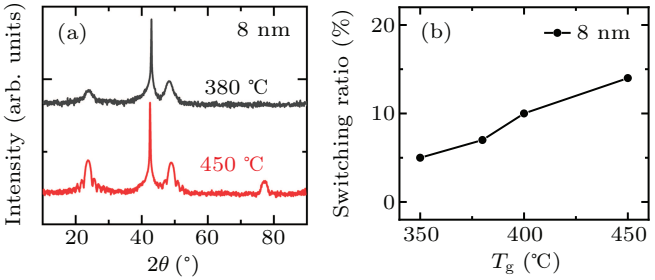


Fig. 3. (a) X-ray diffraction of 8-nm-thick $L1_0$-FePt films grown at 380 °C and 450 °C, (b) variation of magnetization switching ratio with growth temperature for 8-nm-thick FePt film.

Here, we compare the mechanisms of disordering in our previous work[33] with the structural gradient in Ref. [34]. Therefore, we focus on the SOT in 8-nm-thick FePt films with different growth temperatures. We compare the XRD pattern of 8-nm-thick FePt films at $T_g = 380$ °C with that at $T_g = 450$ °C as shown in Fig. 3(a) to calculate the chemical ordering *S*. The values of chemical ordering *S* for $T_g = 380$ °C and $T_g = 450$ °C are 0.45 and 0.83 respectively. The variation trend of magnetization switching ratio for the 3-nm-thick FePt film[33] is opposite to that for the 8-nm-thick sample. On the other hand, the overall changes of the values of magnetization switching ratio with different values of T_g in 8-nm-thick $L1_0$ FePt are not so great as that in 3-nm-thick film. It is believed that more magnetization can be switched in the 8-nm-thick $L1_0$ FePt film with the increase of chemical ordering. Therefore, when the FePt film is thick enough, the structural gradient can

play an important role and the SOT increases with the augment of film thickness and chemical ordering in FePt. On the contrary, the disordering plays an important role in the magnetization switching only for the ultra-thin FePt films.

In order to further study the strength of SOT efficiency, the harmonic Hall voltages of 8-nm-thick $L1_0$ FePt films with different values of T_g are measured with applying AC current of 5 mA in an in-plane magnetic field, and the first and the second voltage signals are detected by using two lock-in amplifiers at the same time. The results of 8-nm-thick $L1_0$-FePt films with $T_g = 380$ °C and $T_g = 400$ °C against in-plane magnetic field $\boldsymbol{H}_x$ are shown in Fig. 4, in which the signals are measured with $\boldsymbol{M}_z > 0$ and $\boldsymbol{M}_z < 0$. The second voltage signals against in-plane magnetic fields $\boldsymbol{H}_y$ for 8-nm-thick $L1_0$-FePt films are too weak to be detected. The damping-like effective field $\boldsymbol{H}_D$ and field-like effective field $\boldsymbol{H}_F$ can be calculated from the following equation:[36–38]

$$H_{D(F)} = -2\frac{H_{L(T)} \pm 2\xi H_{T(L)}}{1 - 4\xi^2}, \tag{1}$$

where ξ is the ratio of planar Hall effect resistance to anomalous Hall effect resistance, and the planar Hall effect resistance can be gained by the method from Refs. [38,39]. The values of ξ for 8-nm-thick $L1_0$-FePt film with $T_g = 380$ °C and with $T_g = 400$ °C are 0.067 and 0.065, respectively. The $\pm$ signs refer to the magnetization pointing $\pm z$. The $H_{L(T)}$ can be calculated from the following equation:

$$H_{L(T)} = \frac{\partial V_{2\omega}/\partial H_{x(y)}}{\partial^2 V_\omega/\partial H_{x(y)}^2}. \tag{2}$$

After the calculations, H_D and H_F for 8-nm-thick $L1_0$-FePt films with $T_g = 380$ °C are 0.43 Oe and 0.06 Oe respectively. H_D and H_F for 8-nm-thick $L1_0$ FePt films with $T_g = 400$ °C are 0.67 Oe and 0.09 Oe respectively. As the growth temperature increases, both H_D and H_F for 8-nm-thick $L1_0$-FePt film increase. However, their effective fields of this magnitude are too small to fully explain the magnetization switching of $L1_0$-FePt. The results from the method of deriving the effective spin torque fields in the previous studies cannot fully explain the spin current generation and self-induced SOT in $L1_0$-FePt single layer.[33,34] Therefore, many factors can influence the SOT in $L1_0$-FePt single layer, and the two mechanisms cannot fully explain the real magnetization switching or spin current generation.[33,34] Here, we emphasize the bulk nature of strong SOC in $L1_0$-FePt through density functional theory calculations, which should generate large spin current due to SHE even the process of magnetization switching will also be influenced by complicated factors such as disorder, interfacial strain and structural gradient.

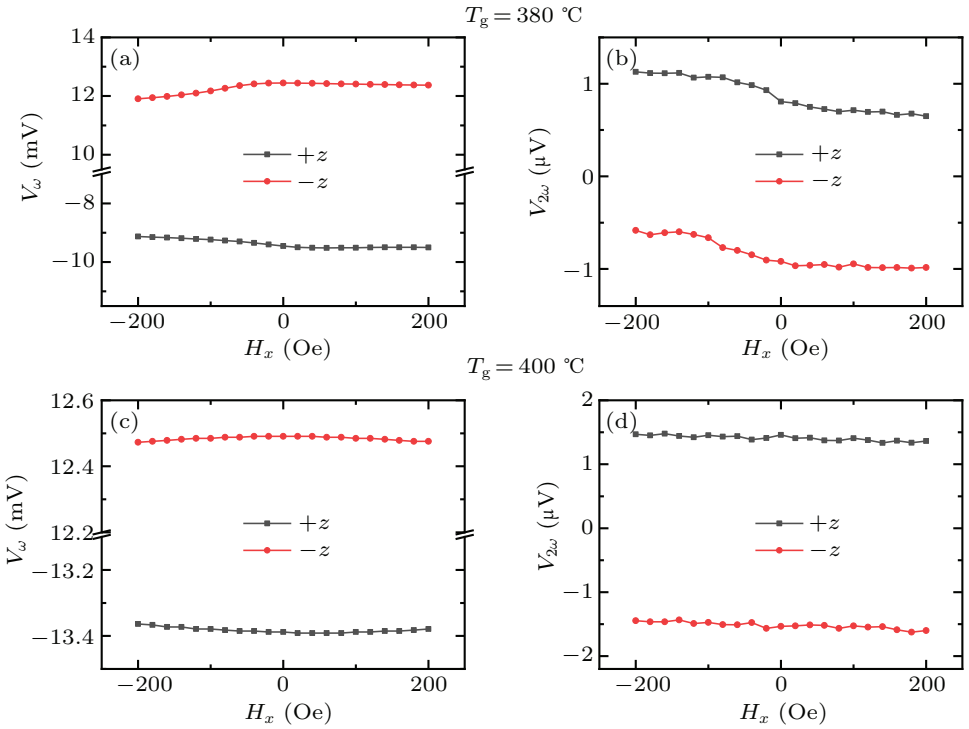


Fig. 4. Plots of first V_ω and second $V_{2\omega}$ harmonic Hall voltages against small in-plane external field H_x in FePt films with $T_g = 380$ °C [(a), (b)] and 400 °C [(c)–(d)]. The black and red signals are measured with out-of-plane magnetization component $M_z > 0$ and $M_z < 0$, respectively.

Our density functional theory calculations are performed by employing the Vienna *ab initio* simulation package (VASP)[40] through using the projected augmented wave (PAW) method.[41] The generalized gradient approximation (GGA) of Perdew–Burke–Ernzerhof (PBE) parametrization for the exchange-correlation functional[42,43] is adopted. The cutoff energy of 450 eV is used for plane wave expansions of electron wave functions. During structure optimizations, all

atoms are fully relaxed until the Hellmann–Feynman forces on them along each direction are less than 0.01 eV/Å. The iron $3d^6 4s^2$ and platinum $5d^9 6s^1$ electrons are treated as valence electrons. The 30×30×30 Monkhorst–Pack[44] k-point meshes are employed for integration over the Brillouin zones of primitive cell. We focus on FePt in the chemically ordered $L1_0$ phase (space group $P4/mmm$). The calculated lattice constants of FePt are $a = b = 3.86$ Å and $c = 3.77$ Å, respectively, which are in good agreement with the experimental values of 3.94 Å and 3.76 Å. In our calculations, the assumption is made that the ground state of FePt is ferromagnetic phase, and the magnetization is contributed from Fe atom. The calculated magnetization is 3.268 μ_B/Fe, which is consistent with the experimental result. The electronic band structures of ferromagnetic FePt along the high-symmetry direction of the Brillouin zone are calculated. Figure 5(a) shows the obtained band structures with the SOC neglected, while figure 5(b) represents the band structures including SOC based on the parameter in VASP. The Fermi energy E_F is set to be zero, and indicated by a gray line. As shown in Fig. 5, the Fermi surface of FePt is mainly formed by Fe 3d states. Comparing Fig. 5(a) with Fig. 5(b), it is not difficult to find that under the effect of SOC, the degeneracy of the energy band near the high symmetry points Z, M, R, and X are all remarkably reduced, and the energy band splits obviously. For example, at M point, the spin orbit splitting is about 0.17 eV. It can be seen from Fig. 5(b) that multiple energy bands cross the Fermi surface, and the Fermi surface of 3D Brillouin zone is very complex. However, owing to the SOC, $3d_{z^2}$, $3d_{xz}$, and $3d_{yz}$ orbitals make the most significant contributions near the Fermi surface. At R point, the $3d_{z^2}$ orbit forms a hole pocket; At X point, the $3d_{yz}$ orbit forms an electron pocket; and the energy bands of $3d_{xz}$ and $3d_{z^2}$ cross the Fermi surface at R point and M point, respectively. Therefore, it is clear that the SOC effect is very strong in FePt.

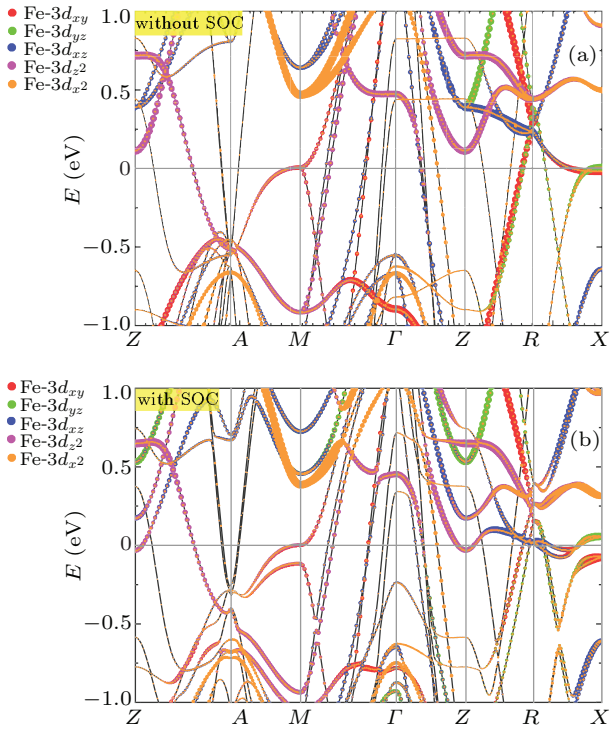


Fig. 5. Band structures of $L1_0$-FePt based on density functional theory calculations.

4. Conclusions

In summary, we have investigated the thickness dependent SOT in $L1_0$-FePt single layers. Comparing with 3-nm-thick $L1_0$-FePt film, much magnetization can be switched in 8-nm-thick $L1_0$-FePt films with the increase of chemical ordering. When the FePt film is thick enough, the SOT in FePt is closely related to the $L1_0$-ordered structure, which displays a bulk nature. However, the switching ratio decreases with thickness further increasing, indicating that more factors should be taken into consideration for SOT of single $L1_0$-FePt film. Although the disordering plays an important role in the magnetization switching only for the ultra-thin FePt films and the structural gradient may play an important role for thicker films, the two mechanisms cannot fully explain the process of magnetization switching or the spin current generation. Finally, we highlight the bulk nature of strong SOC in $L1_0$-FePt through density functional theory calculations. Therefore, a large spin current can be generated from $L1_0$-FePt film due to SHE.

Acknowledgment

We would like to thank Dr. Qi Liu in Southern University of Science and Technology for XRD and XRR characterizations.

References

[1] Manchon A, Železný J, Miron I M, Jungwirth T, Sinova J, Thiaville A, Garello K and Gambardella P 2019 *Rev. Mod. Phys.* **91** 035004
[2] Miron I M, Garello K, Gaudin G, Zermatten P J, Costache M V, Auffret S, Bandiera S, Rodmacq B, Schuhl A and Gambardella P 2011 *Nature* **476** 189
[3] Liu L Q, Lee O J, Gudmundsen T J, Ralph D C and Buhrman R A 2012 *Phys. Rev. Lett.* **109** 096602
[4] Liu L Q, Pai C F, Li Y, Tseng H W, Ralph D C and Buhrman R A 2012 *Science* **336** 555
[5] Meng K K, Miao J, Xu X G, Wu Y, Zhao X P, Zhao J H and Jiang Y 2016 *Phys. Rev. B* **94** 214413
[6] Fukami S, Zhang C L, DuttaGupta S, Kurenkov A and Ohno H 2016 *Nat. Mater.* **15** 535
[7] Cai K, Zhu Z, Lee J M, Mishra R, Ren L, Pollard S D, He P, Liang G, Teo K L and Yang H 2020 *Nat. Electron.* **3** 37
[8] Shao Q, Tang C, Yu G, Navabi A, Wu H, He C, Li J, Upadhyaya P, Zhang P, Razaci S A, He Q L, Liu Y, Yang P, Kim S K, Zheng C, Liu Y, Pan L, Lake R K, Han X, Tserkovnyak Y, Shi J and Wang K L 2018 *Nat. Commun.* **9** 3612
[9] Nishimura T, Kim D Y, Kim D H, Nam Y S, Park Y K, Kim N H, Shiota Y, You C Y, Min B C, Choe S B and Ono T 2021 *Phys. Rev. B* **103** 104409
[10] Hirsch J E 1999 *Phys. Rev. Lett.* **83** 1834

[11] Murakami S, Nagaosa N and Zhang S C 2003 *Science* **301** 1348
[12] Sinova J, Culcer D, Niu Q, Sinitsyn N A, Jungwirth T and MacDonald A H 2004 *Phys. Rev. Lett.* **92** 126603
[13] Kato Y K, Myers R C, Gossard A C and Awschalom D D 2004 *Science* **306** 1910
[14] Miron I M, Gaudin G, Auffret S, Rodmacq B, Schuhl A, Pizzini S, Vogel J and Gambardella P 2010 *Nat. Mater.* **9** 230
[15] Rodmacq B, Manchon A, Ducruet C, Auffret S and Dieny B 2009 *Phys. Rev. B* **79** 024423
[16] Manchon A, Koo H C, Nitta J, Frolov S M and Duine R A 2015 *Nat. Mater.* **14** 871
[17] Miron I M, Garello K, Gaudin G, Zermatten P J, Costache M V, Auffret S, Bandiera S, Rodmacq B, Schuhl A and Gambardella P 2011 *Nature* **476** 189
[18] Liu L, Pai C F, Li Y, Tseng H W, Ralph D C and Buhrman R A 2012 *Science* **336** 555
[19] Grimaldi E, Krizakova V, Sala G, Yasin F, Couet S, Kar G S, Garello K and Gambardella P 2020 *Nat. Nanotechnol.* **15** 111
[20] Zhu L, Zhu L, Shi S, Ralph D C and Buhrman R A 2020 *Adv. Electron. Mater.* **6** 1901131
[21] Demidov V E, Urazhdin S, Ulrichs H, Tiberkevich V, Slavin A, Baither D, Schmitz G and Demokritov S O 2012 *Nat. Mater.* **11** 1028
[22] Luo Z, Hrabec A, Dao T P, Sala G, Finizio S, Feng J, Mayr S, Raabe J, Gambardella P and Heyderman L J 2020 *Nature* **579** 214
[23] Ou Y, Shi S, Ralph D C and Buhrman R A 2016 *Phys. Rev. B* **93** 220405
[24] Pesin D A and MacDonald A H 2012 *Phys. Rev. B* **86** 014416
[25] Chi Z, Lau Y C, Xu X, Ohkubo T, Hono K and Hayashi M 2020 *Sci. Adv.* **6** 2324
[26] Fan X, Wu J, Chen Y, Jerry M J, Zhang H and Xiao J Q 2013 *Nat. Commun.* **4** 1799
[27] Fan X, Celik H, Wu J, Ni C, Lee K J, Lorenz V O and Xiao J Q 2014 *Nat. Commun.* **5** 3042
[28] Chernyshov A, Overby M, Liu X, Furdyna J K, LyandaGeller Y and Rokhinson L P 2009 *Nat. Phys.* **5** 656
[29] Yoshimi R, Yasuda K, Tsukazaki A, Takahashi K S, Kawasaki M and Tokura Y 2018 *Sci. Adv.* **4** eaat9989
[30] Trichy G R, Chakraborti D, Narayan J and Prater J T 2008 *Appl. Phys. Lett.* **92** 102504
[31] Tsai W C, Liao S C, Huang K F, Wang D S and Lai C H 2013 *Appl. Phys. Lett.* **103** 252405
[32] Xu S J, Shi Z and Zhou S M 2018 *Phys. Rev. B* **98** 024413
[33] Zheng S Q, Meng K K, Liu Q B, Chen J K, Miao J, Xu X G and Jiang Y 2020 *Appl. Phys. Lett.* **117** 242403
[34] Tang M, Shen K, Xu S J, Yang H L, Hu S, Lü W M, Li C J, Li M S, Yuan Z, Pennycook S J, Xia K, Manchon A, Zhou S M and Qiu X P 2020 *Adv. Mater.* **32** 2002607
[35] Christodoulides J A, Farber P, Daniil M, Okumura H, Hadjipanayis G C, Skumryev V, Simopoulos A and Weller D 2001 *IEEE Trans. Magn.* **37** 1292
[36] Hayashi M, Kim J, Yamanouchi M and Ohno H 2014 *Phys. Rev. B* **89** 144425
[37] Lee H R, Lee K, Cho J, Choi Y H, You C Y, Jung M H, Bonell F, Shiota Y, Miwa S and Suzuki Y 2014 *Sci. Rep.* **4** 6548
[38] Meng K K, Miao J, Xu X G, Wu Y, Zhao X P, Zhao J H and Jiang Y 2017 *Appl. Phys. Lett.* **110** 142401
[39] Qiu X, Narayanapillai K, Wu Y, Deorani P, Yang D H, Noh W S, Park J H, Lee K J, Lee H W and Yang H 2015 *Nat. Nanotechnol.* **10** 333
[40] Kresse G and Furthmuller J 1996 *Phys. Rev. B* **54** 11169
[41] Kresse G and Joubert D 1999 *Phys. Rev. B* **59** 1758
[42] Perdew J P, Burke K and Ernzerhof M 1996 *Phys. Rev. Lett.* **77** 3865
[43] Perdew J P, Burke K and Ernzerhof M 1998 *Phys. Rev. Lett.* **80** 891
[44] Monkhorst H J and Pack J D 1976 *Phys. Rev. B* **13** 5188